Irina Statnaia [1,2], Alexey Karpechko[2], Heikki Järvinen[1]

[1] University of Helsinki, Institute for Atmospheric and Earth System Research

[2] Finnish Meteorological Institute, Polar Meteorology and Climatology group

HELSINGIN YLIOPISTO

Mechanisms and predictability of Sudden Stratospheric Warming in winter 2018

1. Background

Sudden Stratospheric Warming (SSW) - an event in which the zonal mean zonal winds at 10 hPa and 60°N reverse to easterly (i.e. negative) from Nov to Mar; the stratospheric temperature rises by several tens of Kelvins over the course of a few days. Such anomalous events are one of the key sources of predictability in wintertime. Here we consider ECMWF 51-member ensemble forecast initialized on Feb 1 of an SSW that occurred in February 2018.

SSW 2018

- Central date: Feb 12
- Only 25% of ensemble members predicted the wind reversal with the lead time of 12 days (Fig. 1)
- Planetary wave 1 (PW1) dominates on Feb 1 (Fig. 2)
- On Feb 5 amplitude of PW2 starts to grow, while PW1 amplitude decreased (Fig. 2)

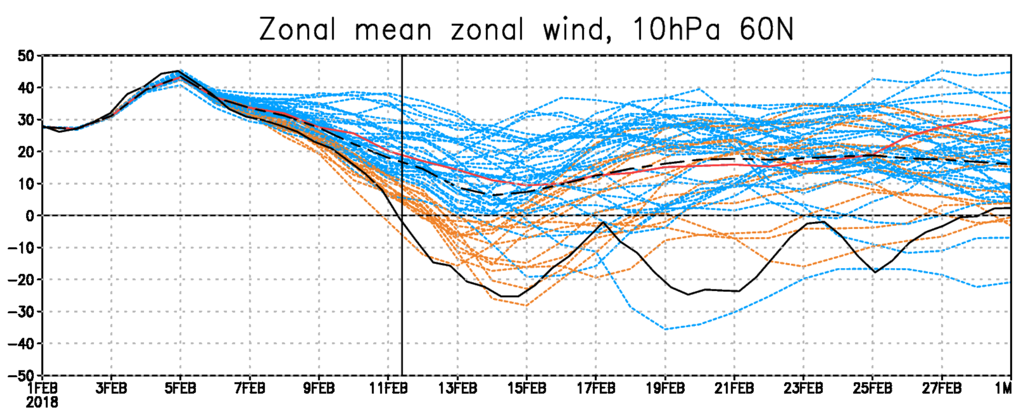

Fig. 1 Zonal mean zonal wind at 10 hPa 60°N. Ensemble forecast initialized on Feb 1 (orange lines denote ensemble members that predict wind reversal with max 1 day delay, red line – control fc, black dashed line – ensemble mean) and ERA-Interim re-analysis (black solid line). Vertical line denotes SSW2018 central date

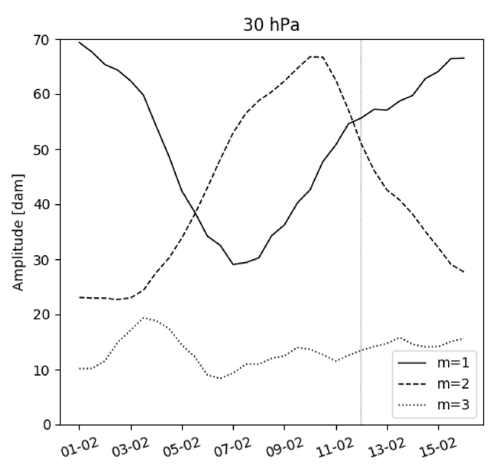

Fig. 2 Time series of amplitudes of planetary waves with zonal wavenumbers m=1,2 and 3 in geopotential height (dam) at 30 hPa averaged over the latitudinal belt 40°-75°N, ERA-Interim re-analysis. Vertical line denotes SSW2018 central date

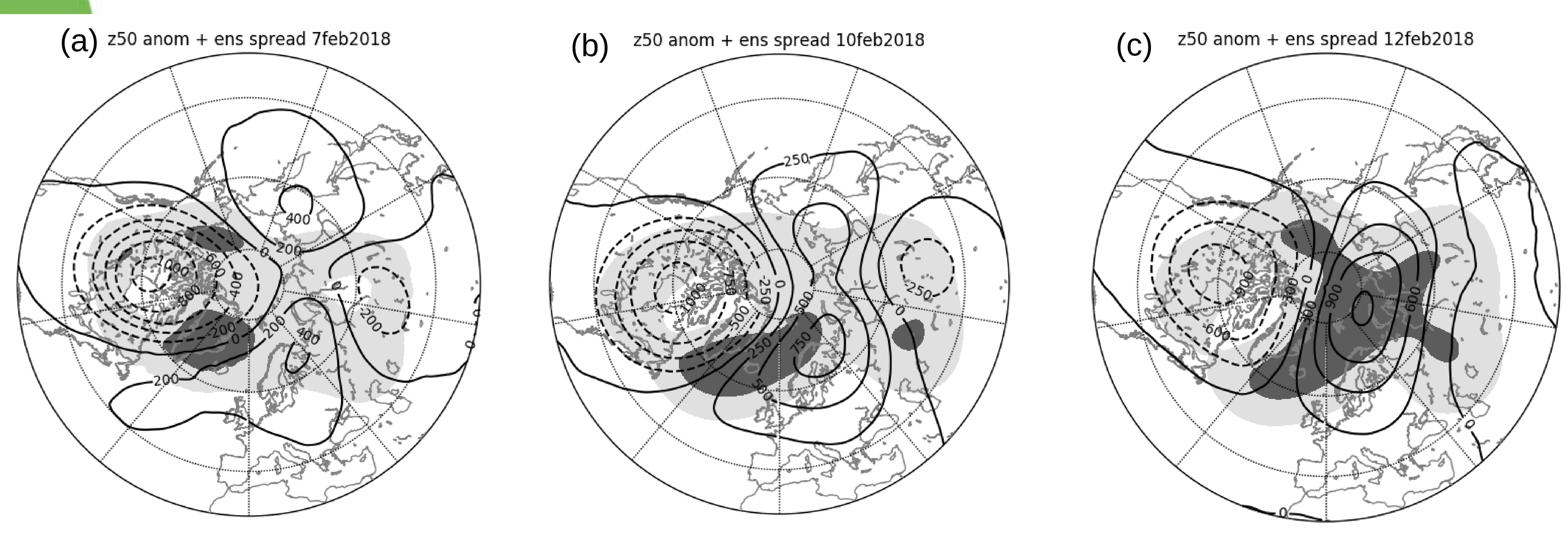

Fig. 3 ERA-Interim 50-hPa geopotential height anomaly (contours) with respect to the 1979-2017 climatology and ensemble spread predicted for (a) 7th, (b) 10th, (c) 12th February 2018 (shaded lightly and heavily for 0.3-0.6 values and values greater than 0.6, respectively). The spread has been normalized by minimum and maximum values within the domain north of 20N.

The largest ensemble spread on Feb 7 is mainly confined to the subpolar North Atlantic (Fig. 3 a). Throughout the period of vortex deceleration the area of the large forecast spread at 50 hPa height gradually expands horizontally and by 12th February it covers most of the polar stratosphere north of 70N (Fig. 3 b,c).

- On Feb 7 there are 3 areas of large ensemble-forecast spread: over Ural, Alaska and North Atlantic regions. These regions are associated with anticyclonic anomalies that act as the source of upward propagating Rossby-wave packets (Fig. 4).
- Geopotential anomaly lines tilt westward with height which indicates the upward group velocity propagation of the Rossby wave packets (Fig. 4).

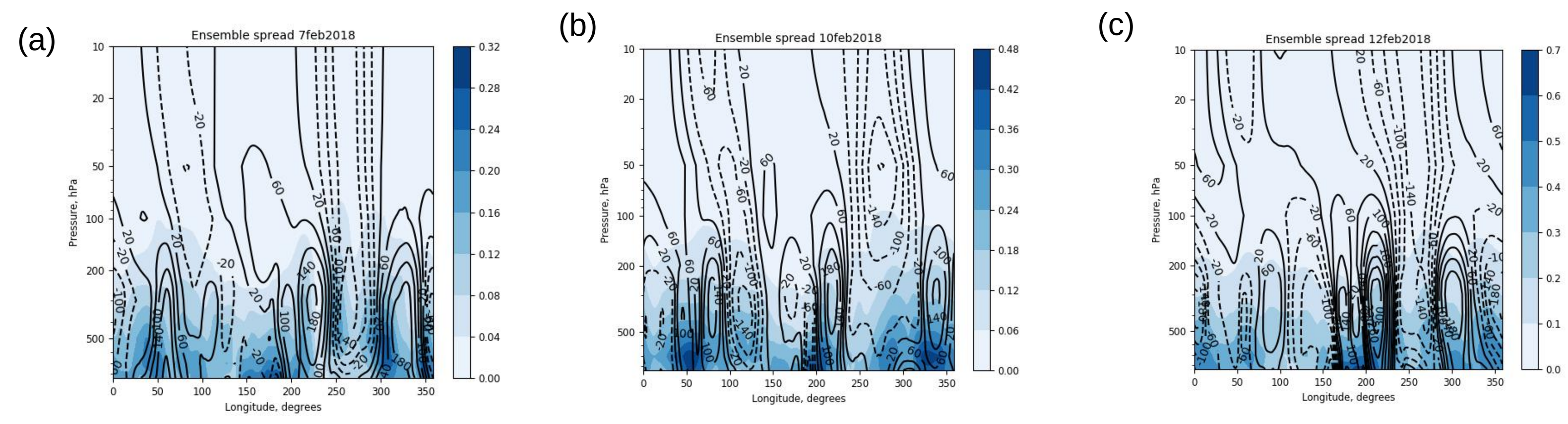

Fig. 4 Zonal cross-sections for 50°N of the ensemble spread of geopotential height predicted for (a) 7th, (b) 10th, (c) 12th February 2018. Superimposed contours represent observed geopotential anomalies with respect to the 1979-2010 climatology. Spread and anomaly are normalized by pressure.

- Downstream development is seen in the 250 hPa geopotential height (Fig. 5a). The wave packet associated with meandering westerlies emerged on Feb 3 over the North Atlantic and then propagated downstream until blocked by the developing anticyclonic ridge over the Ural region around Feb 7.
- The second ridge over the North Atlantic begins to develop on Feb 4.
- A stationary upper troposphere ridge is seen over Alaska over the whole period.
- Observed max of the squared 250 hPa meridional wind (Fig. 5 b) associated with the two wave packets exhibits a signature of group velocity propagation across the North Atlantic and Northern Eurasia on 3-8 Feb. Group velocity is ~27° in longitude per day, phase speed is ~10° per day which correspond to a baroclinic wave packet.
- The forecast spread shown in meridional wind at 250 hPa (Fig. 5 c) also indicates the two distinctive areas of forecast errors which correspond to wave packets.

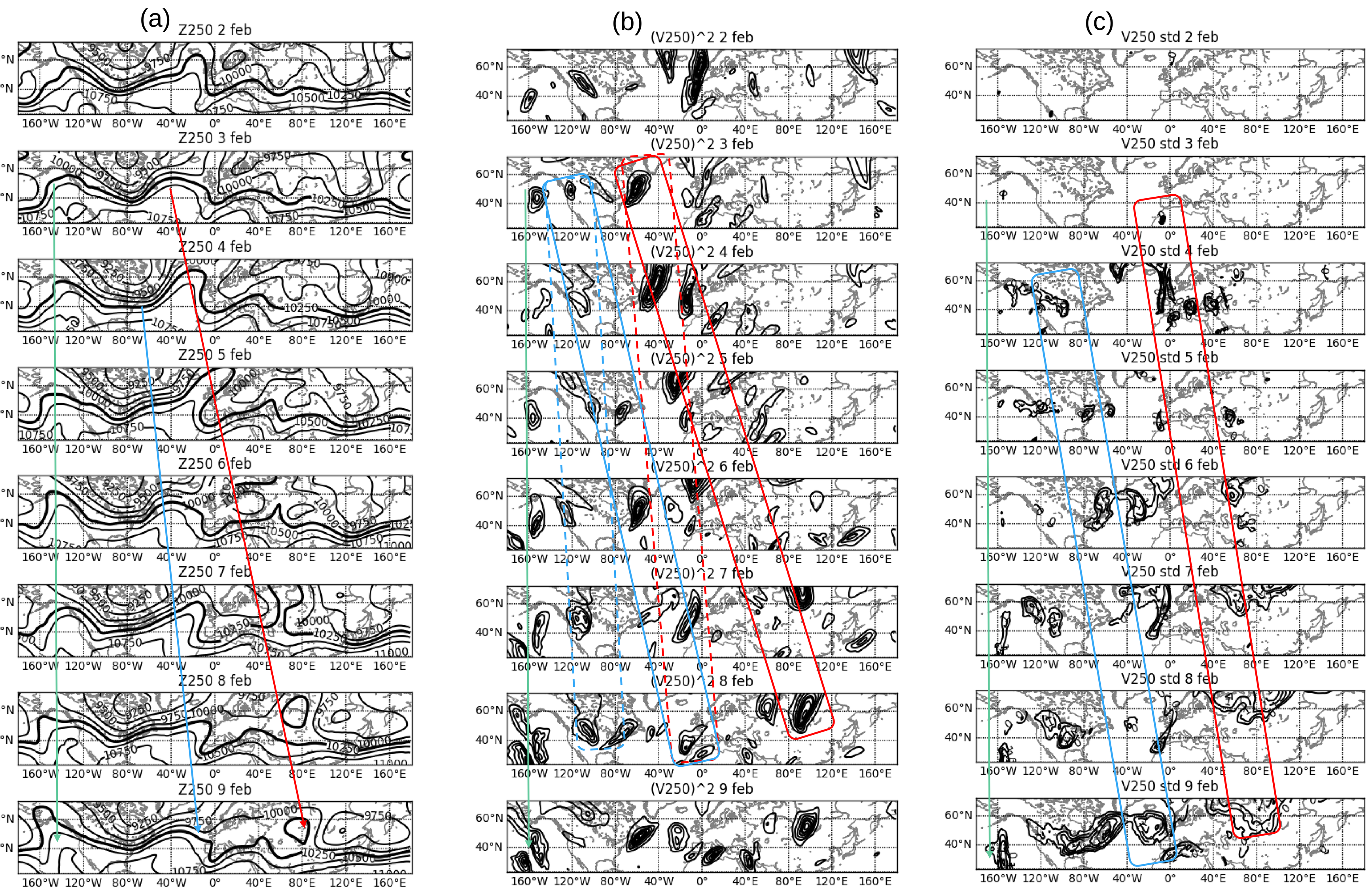

Fig. 5 (a) Time sequence of 250 hPa geopotential height observed from (top) 2nd to (bottom) 9th February 2018 over a domain (20°N-70°N). The thick contour corresponds to 10250 m. (b) 250 hPa meridional velocity squared. (c) standard deviation of predicted 250 hPa meridional wind velocity among ensemble members for the initial date of 1 February 2018. The standard deviation is normalized by maximum and minimum within the domain. Contour intervals are 0.1 starting from 0.5.

2. Teleconnection with MJO

It has been shown that MJO phase 6/7 events associated with OLR anomalies in Eastern Pacific can lead to weakening of the polar vortex thorough enhancement of upward propagating wave fluxes towards Alaska and are often followed by SSWs (Schwartz et al., 2017).

In the end of January the amplitude of MJO phase 6 was large and the OLR anomalies extended into the South China Sea.

⬇

By the Feb 1 the MJO induced wave packets might have been already present in the atmosphere.

To discern the error in wave fluxes we selected two groups of ensembles:

- 10 'good' ensemble members that forecasted wind reversal with max 1 day delay
- 10 'bad' ensemble members that maintained high positive values of U10 at 60°N (Fig.1)

(a)

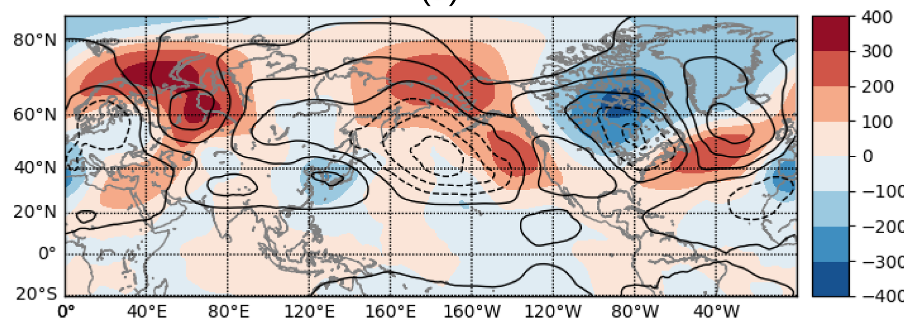

Fig. 6 Composite anomalies of geopotential height picked only for days with MJO phase 6 with averaged lag of 5-9 days at 500 hPa (contours) and anomalies of geopotential height at the same level averaged over Feb 5-7 (shaded). (a) ERA-I, composites calculated using 1980-2010 data, (b) 'good' ensemble members, composites calculated using hindcasts over 20 years (1997-2017), (c) same as in (b), but for 'bad' ensemble members.

(b) (c)

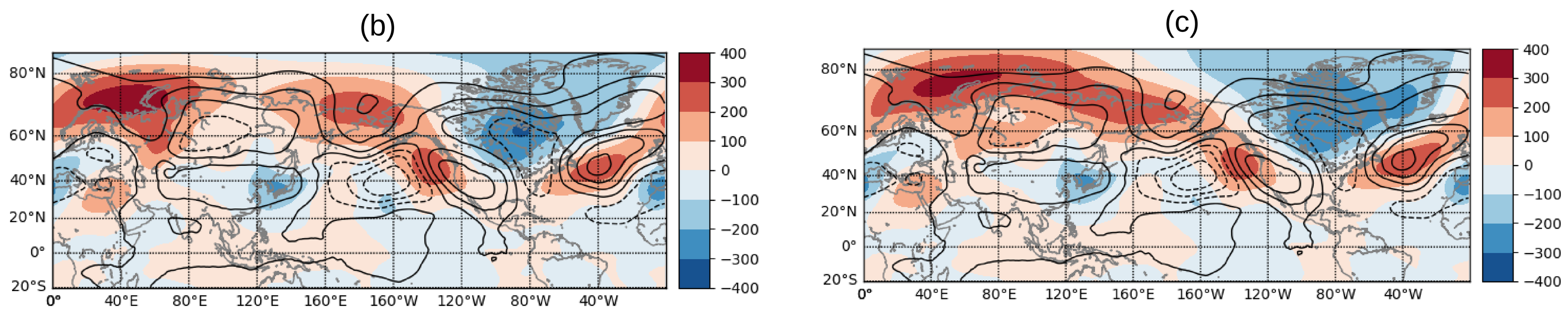

- Composite field that shows fingerprint of MJO phase 6 corresponds greatly to the field observed on Feb 5-7
- 'Good' ensemble members managed to capture the structure of geopotential field with PW2 prevailing in northern latitudes, and strongly resembles MJO composite
- PW1 is clearly seen in 'bad' group of ensemble members and it does not resemble nether observed field nor the MJO composite with two highs in Alaska and Ural region blended together

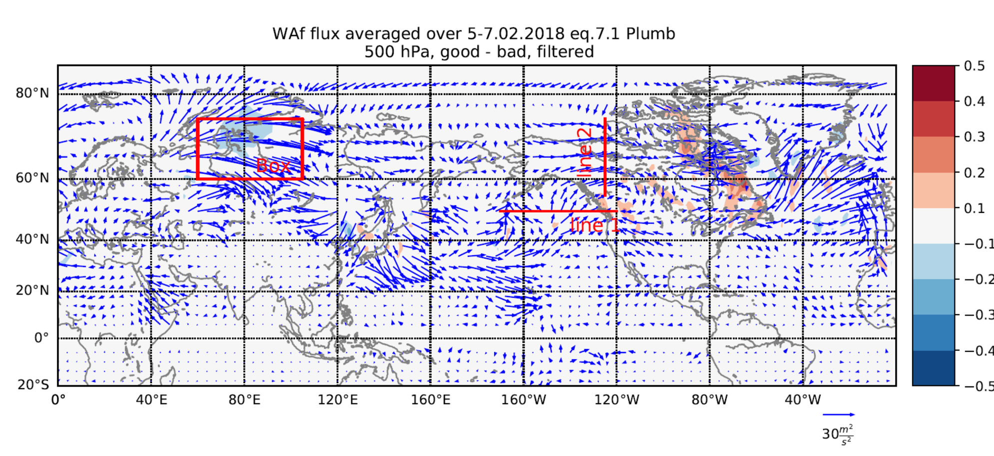

Fig. 7 Difference in wave activity flux at 500 hPa averaged over Feb 5-7 between good and bad ensemble members. Vectors show horizontal flux ($m^2 s^{-2}$), colours denote vertical component.

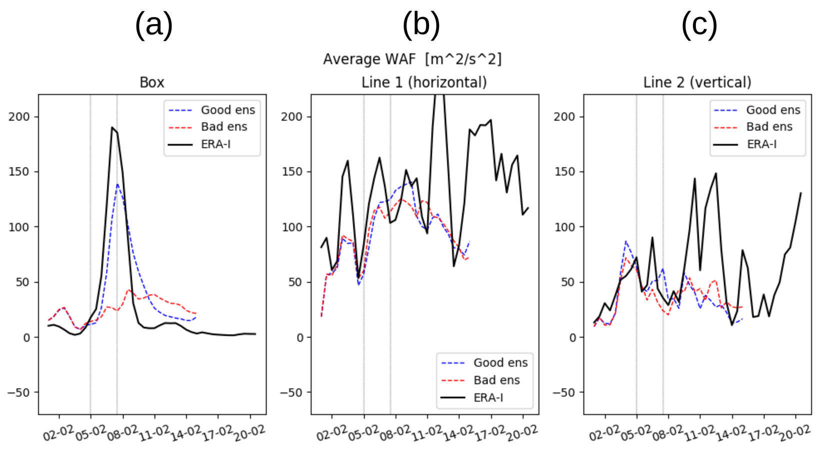

Fig. 8 Time series of wave activity flux at 500 hPa averaged over the Box and through the Line 1 and 2 shown in Fig. 7. Units are $m^2 s^{-2}$. Grey vertical lines denote Feb 5 and Feb 7.

- Wave activity within the box is significantly higher across 'good' ensemble members, though it is less than in the ERA-Interim verification (Fig. 8 a)
- The wave activity fluxes through the surfaces defined by the lines 1 and 2 (Fig. 8 b,c) are comparable within 'good' and 'bad' ensemble members but also underestimate values obtained with ERA-Interim
- Wave fluxes within the box support the idea of downstream development of the Ural blocking high

3. Summary

- Two tropospheric anticyclones (over the North Atlantics and North Pacific) acted as the sources of upward propagating wave packets
- These two regions correspond to the largest forecast spread
- The anticyclonic centres over Northern Atlantic, Ural and Alaska regions formed prior to the SSW2018 correspond to the MJO phase 6 response pattern
- The anticyclonic centres were captured well by the 'good' ensemble members while the 'bad' ensembles failed to reproduce the PW2 structure in the northern latitudes
- The main difference in wave activity fluxes between 'good' and 'bad' ensemble members can be seen in the Ural region. The amount of the wave energy propagating in this area and leading to a blocking anticyclone formation is underestimated by the 'bad' ensemble members

References:

Karpechko, A. Yu. & Charlton-Perez, A. & Balmaseda, M. & Tyrrell, N. & Vitart, F. (2018). Predicting Sudden Stratospheric Warming 2018 and Its Climate Impacts With a Multimodel Ensemble. Geophysical Research Letters. 10.1029/2018GL081091.

Schwartz, C. and C. I. Garfinkel (2017), Relative roles of the MJO and stratospheric variability in North Atlantic and European winter climate, J. Geophys. Res. Atmos., 122, 4184–4201, doi:10.1002/2016JD025829.

Contact:
Irina Statnaia
irina.statnaia@helsinki.fi